Influence of the Slag Composition on the Fluorine Absorption in γ-TiAl during IESR

P. Spiess[1], B. Friedrich[1]
[1]IME Process Metallurgy and Metal Recycling, RWTH Aachen University, D-52056 Aachen, Germany

Keywords: TiAl, Recycling, IESR, Halogen Effect, Fluorine, Slag System, Oxidation Resistance

Abstract

Because of the oxidation resistance of γ-TiAl-alloys the long term use is limited to temperatures up to 700 °C. In literature, it has been reported that the so called halogen effect has an outstanding improvement on the oxidation resistance of γ-TiAl. This implication is based on the forming of gaseous Al-halides which are oxidized to Al_2O_3 on the surface resulting in a protective alumina scale.

To investigate the absorption of fluorine in γ-TiAl during electroslag remelting and to enhance the oxidation resistance of the produced alloy by bulk-fluidization a series of tests was performed at IME. Hence, in a 400 kW lab scale furnace multiple electrodes of Ti-45Al were remelted by using a CaF_2 flux. The slag composition was varied by partially substitution of CaF_2 with MgF_2. The alloys as well as the slag were analyzed on their composition to set up the fluorine content by influencing the melting parameters.

Introduction

Due to the rapidly increasing global transport capacity with an annual 5 % growth of revenue passenger kilometers (RPK; cf. Figure 1) [1], CO_2 emissions generated by aviation have reached new heights of 650 million tons per year. [2] Relief could be produced by the substitution of heavy superalloys by structural intermetallic alloys whose development for industrial use has been a focus since the 1980s: the group of titanium aluminides. They are characterized by eminent properties like low density (3.9 – 4.1 g/cm³), high melting point (about 1450 °C), high specific creep resistance (39 – 46 GPa cm³ g^{-1}), high specific elasticity modulus and good oxidation resistance up to 700 – 800 °C. Due to the steady increasing use of TiAl in combustion engines as an alternative to superalloys, pollutant emissions as well as fuel consumption can be reduced significantly. [2-4] Because of confidentiality reasons, no precise information on the TiAl content in combustion engines is available.

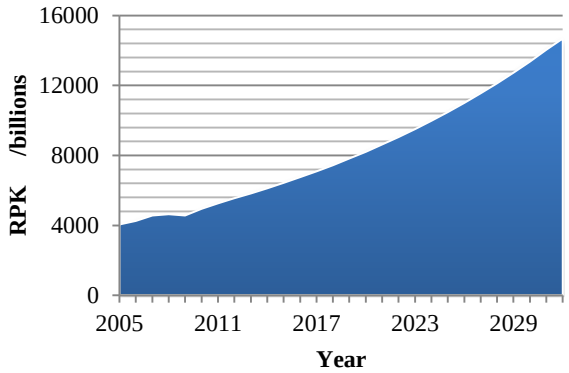

Figure 1: Revenue Passenger Kilometers (RPK) outlook 2013-2032 with an annual growth of 5 % [1]

In addition to the substitution of superalloys by titanium aluminides in the low pressure turbine (LPT), a further increase of the efficiency of combustion engines can be achieved by raising their operating temperature. However, one must consider that operating temperatures above 800 °C lead to a considerable drop of the oxidation resistance of TiAl, due to the formation of a mixed Al_2O_3-TiO_2 oxide layer. The oxides have different rates of growth and expansion coefficients resulting in crack formation in the oxide layer. Since niobium lowers the Al activity, by the addition of small amounts niobium the oxidation resistance can be increased. Thereby, a finer grain structure and a change of the kinetics of flaking are achieved, given that niobium is attached to the Ti sub-lattice of α_2-Ti_3Al and γ-TiAl structure. However, the addition of niobium is limited to about 2 wt.-% due to a massive drop of Al activity preventing the formation of Al_2O_3. Consequently, the oxygen diffusion is accelerated given that TiO_2 is a weak oxygen barrier. [5-6]

According to Schütze [6] a further increase of the oxidation resistance can be realized by microalloying of halogens like bromine, chlorine, fluorine or iodine. Based on the so called "halogen effect", small amounts of halogens are implanted into the alloy surface, whereas Donchev [7-8] observed, that a sustained increase in oxidation resistance can only be achieved by fluorine. Fluorine deposited in the metal edge zone selectively forms Al-fluorides at high temperatures, which shift through pores and microcracks to the metal surface. Due to the increasing oxygen partial pressure the fluorides decay and form gaseous F_2 and a dense Al_2O_3 layer. [9]

IME developed a TiAl recycling process consisting of multiple industry approved processes which is explicitly explained by Reitz [10]. It is based on the deoxidization of via vacuum induction melting (VIM) consolidated casting scrap by pressure electroslag re-melting (PESR) with a subsequent optional vacuum arc remelting (VAR) step. To achieve a designated refining and deoxidization of the metal during PESR a reactive slag consisting of CaF_2 and metallic Ca is used. Due to its low vapour pressure, physical properties and good availability Nafziger [11] identified CaF_2 as the most suitable flux for ESR of titanium and titanium alloys. Because of the thermodynamic effects during ESR of titanium at high temperatures of around 1800 °C, CaF_2 decomposes (cf. eq. 1). By reaction of existant atomic fluorine radicals with the liquid metal, titanium fluorine TiF is formed (cf. eq. 2) and dissolves in the melt subsequently (cf. eq. 3).

$$(CaF_2) = \{CaF\} + \{F\} \quad \text{with } \Delta G_{R,1} \qquad (1)$$

$$(Ti) + \{F\} = \{TiF\} \quad \text{with } \Delta G_{R,2} \qquad (2)$$

$$\{TiF\} = [TiF]_{Ti} \quad \text{with } \Delta G_{R,3} \qquad (3)$$

After ESR of titanium minor amounts of fluorine of about 60 ppm are unavoidable, whereby the fluorine pickup can be influenced by the slag composition (cf. Table I) [11-12]. To obtain a positive

effect of the F-effect on the oxidation resistance, an expected fluorine content of up to 500 ppm is needed.

Table I: Fluorine pickup in electroslag melted titanium as a function of fluoride slag composition [11]

Slag composition	Fluorine pickup /ppm
Native fluorspar (CaF_2)	< 50
Reagent-grade fluorspar (CaF_2)	75
Acid-grade fluorspar (CaF_2)	140
4 wt.-% MgF_2-CaF_2	90
12 wt.-% MgF_2-CaF_2	110
Magnesium fluoride (MgF_2)	300
Barium fluoride (BaF_2)	50
Lanthanum trifluoride (LaF_3)	78

Previous investigations [13] have shown, that the use of both a pure and an active CaF_2 slag leads to no significant fluorine enrichment and thereby no positive effect on the halogen effect when remelting titanium aluminides. However, no deposition of CaF_2 on the grain boundaries was observed. Regarding the thermal stability of CaF_2 the present work gives attention to the partial substitution of the slag with MgF_2, whereby higher fluorine absorption is aspired.

Experimental

According to the tending fluorine pickup in titanium given in Table I, the influence of the slag composition on the fluorine absorption was investigated. Therefore, multiple remelting trials with a specific variation of the slag composition were performed. The experiments were conducted at IME Process Metallurgy and Metal Recycling, Department and Chair of RWTH Aachen University.

Electro**S**lag **R**emelting Furnace (ESR)

In 1958, the construction of the first commercial ESR furnace was finished at the Dneprospetsstal works. It was based on the method of electro-slag welding (ESW) and developed by Slavyanow at the E.O. Paton Institute of Electric Welding in the 1880s. [14] An overview of the basic operating mode of ESR gives the subsequent Figure 2.

The electroslag re-melting process is based on a self-consumable electrode that is gradually molten by contact with a defined liquid slag. The molten metal drips from the electrode and sinks through the slag bath while solid, non-metallic inclusions with a melting temperature higher than that of the base-metal will float into the slag. Certainly, this float will only take place if the inclusions possess a density that is lower than that of the base-metal. Depending on the chemical properties and density of the inclusions they can be dissolved in the slag. The dripping metal solidifies partly directional in a water cooled copper crucible (cf. Figure 3). [13, 16]

Experimental Setup

The investigations where performed in the IME pressure electroslag remelting furnace that is controlled by means of computer-aided software (cf. Figure 4). The furnace is capable to remelt electrodes with a maximum length of 1340 mm and a diameter of up to 110 mm. The available water-cooled molds have a height of up to 900 mm and an inner diameter of about 170 mm.

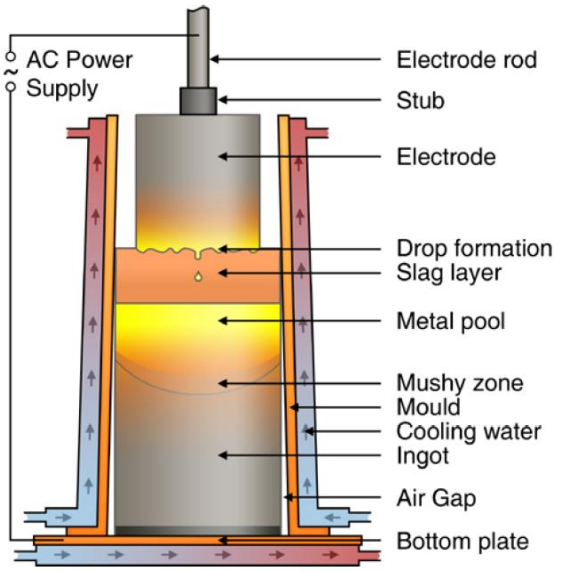

Figure 2: Principle design of a state-of-the-art electroslag remelting furnace [15]

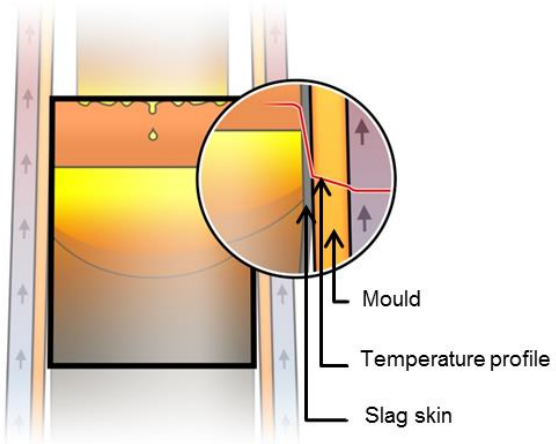

Figure 3: Heat removal by water cooled copper mould during the ESR process [15]

Figure 4: IME **P**ressure **E**lectro**S**lag **R**emelting furnace (PESR)

The remelting chamber consists of a closed system that can be used at atmospheric pressure or pressures up to 50 bars. The power supply is carried out by a thyristor control, where an operating voltage of 80 V and a current of 5 kA, 66.6 V and 6 kA respectively can be tapped. Both cases result in a maximum power output of approximately 400 kW.

During the experiments, the IME PESR was used in closed state with a pressure of 20 bars. As mold a conical copper mold with a height of 890 mm and a lower diameter of 170 mm was used. For an easy removal of the ingot the upper diameter is 154 mm and the bottom plate is removable. A starting plate made of TiAl sputter targets (cf. Figure 5) is placed on the crucible bottom to ensure electrical contact during the starting phase of the process. Afterwards, the crucible is filled with the process slag that mostly consists of the technically pure CaF_2 slag Wacker Electroflux 2052 (> 97 wt.-% CaF_2).

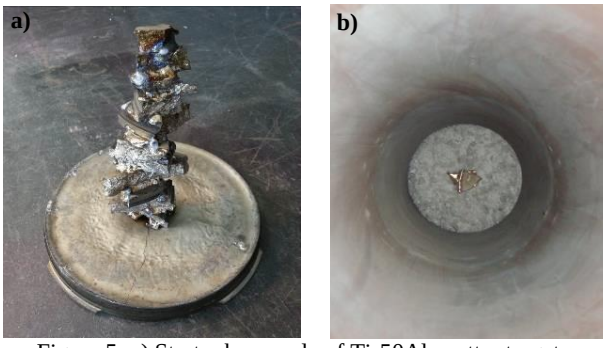

Figure 5: a) Starter box made of Ti-50Al sputter targets
b) Starter box in crucible surrounded by slag

As feedstock, pressed electrodes made of titanium sponge and aluminum rods with a length of 1200 mm and a circumference of 301 mm were used (cf. Figure 6). In order to avoid reactions with oxygen from ambient air the vessel is evacuated to 1^{-10} mbar and backfilled with Ar gas up to the desired process pressure.

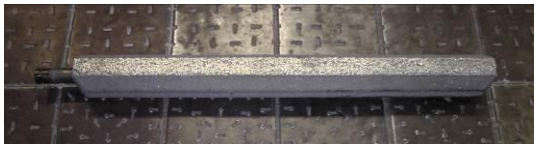
Figure 6: Pressed Ti-45Al electrode made from titanium sponge and aluminum rods

Experimental Procedure

After setting up the furnace, the process starts with an initial phase. During this phase the solid slag is molten and the electrode is preheated to ensure a smooth transition to the melting phase. Thereby, the control of the process at the beginning is done by controlling the current and the voltage and changed to control of power and resistance once the slag is completely molten. After reaching the melting phase the process parameters have been kept constant while the slag system of each experiment was changed to examine the influence of the slag system on the fluorine absorption in Ti-45Al. An overview of the PESR experiments carried out with identical electrodes and the process parameter settings as well as the slag composition used is given in the following Table II.

Table II: Variation of the slag composition of each experiment

Trial	Power /kW	Resistance /mOhm	Slag Composition
Ref.	125.0	9.2	2052 *)
A	125.0	9.2	2052 + 2.5 wt.-% MgF_2
B	125.0	9.2	2052 + 5.0 wt.-% MgF_2
C	125.0	9.2	2052 + 10.0 wt.-% MgF_2

*) Wacker Electroflux 2052 (> 97 wt.-% CaF_2)

As previous investigations have shown (Ref., [13]), a technically pure CaF_2 slag is not sufficient to obtain a traceable fluorine absorption. Therefore, CaF_2 has been substituted by MgF_2 with 2.5, 5.0 and 10.0 wt.-%.

After remelting the obtained ingots were sectioned and sampled at three different heights in the mechanical workshop at IME and characterized by GDOS, GDMS and EDX. The detection limit for fluorine was 0.3 ppm. The slag was milled and sampled (cf. Figure 7) in the chemical lab at IME and characterized by ICP-OES.


Figure 7: Slag sample preparation by milling in a ball mill

Results

During the conventional production of titanium aluminides the homogeneity of the material is an important factor. Therefore, the metal samples were analyzed by GDOS both on titanium and aluminum content on three different heights and three times over the radius at each height. The titanium contents of Trial C are shown in Figure 8 exemplarily. It can be seen that a decrease of the titanium content takes place from bottom to top of the ingot as well as from middle to edge. This effect might be due to the nature of the used electrodes since no change regarding the slag composition was observed. As described in the experimental setup, the electrodes consist of pressed titanium sponge and aluminum rods. By reason of the lower melting temperature of aluminum compared to titanium, the aluminum rods melt down faster resulting in a slight decrease of the titanium content in the remelted ingot. Nevertheless, no explanation concerning the decreasing content over the radius has been found yet. However, it may be noted that the homogeneity of the ingot shows only minor variations of around 0.6 wt.-% and a fine lamellar structure of α_2-Ti_3Al and γ–TiAl.

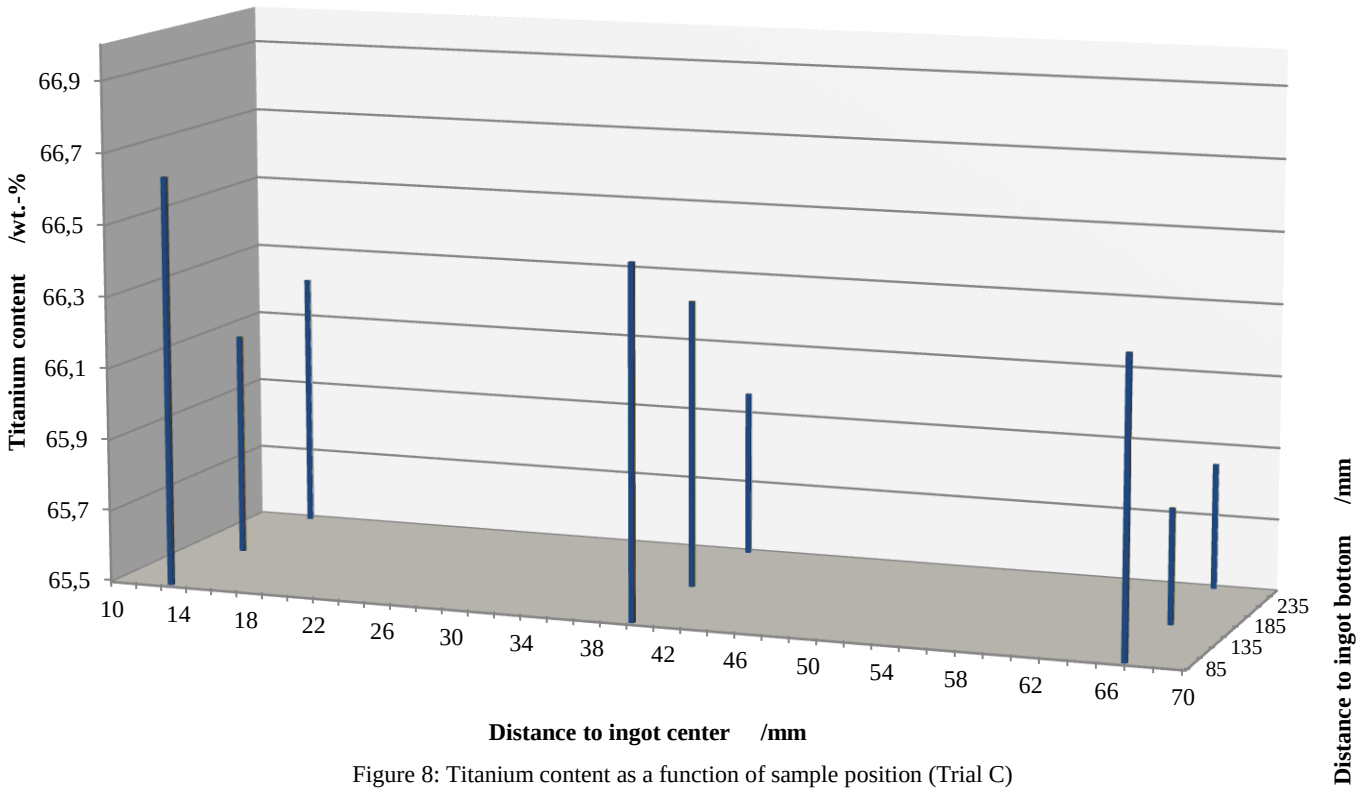

Figure 8: Titanium content as a function of sample position (Trial C)

Since the analysis of the fluorine content has been a challenge in previous investigations due to the detection limit, the samples have been analyzed by GDMS with a detection limit of 0.3 ppm. The results are shown in Figure 9. It can be seen, that a technically pure CaF_2 slag without MgF_2 leads to no detectable fluorine content in the metal. By a partial substitution of 2.5 wt.-% the process slag the fluorine content can be raised to a detectable amount of 0.35 ppm. A further substitution of 5.0 and 10.0 wt.-% respectively leads to a further increase of fluorine in the alloy. Nevertheless, it can be assumed that the fluorine absorption is leveling off if the process slag obtains higher MgF_2 contents. A doubling of the MgF_2 content from Trial A to Trial B results in a rise of the fluorine content of almost 43 %. On the other hand, a doubling of the MgF_2 content from Trial B to Trial C results in a rise of the fluorine content of only 16 %.

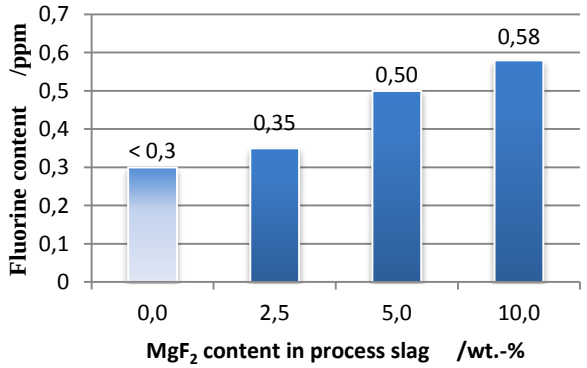

Figure 9: Analyzed fluorine content by GDMS

Due to the process related contact of the alloy system with a process slag, non-metallic inclusions (NMI) might be found in the ingot. Therefore, the material was analyzed by EDX to determine the amount, the size and the composition of possible NMI. Measuring fields with a size of 10.38 x 2.01 mm were determined and are shown in Figure 10 while the results of the analysis are shown in Figure 11. It can be seen, that most of the inclusions have a diameter of 1.0 to 2.5 µm. Considering the oxidic NMI, Figures 11 a), b) and c) show an almost consistent distribution. A correlation between the slag substitution and the amount and size of oxidic NMI (cf. Figure 11 d)) cannot be seen. Nevertheless, there is a correlation between the slag composition and the fluoridic NMI. Trial A (cf. Figure 11 a)) shows an almost equal distribution of CaF_2 and $CaF_2 + MgF_2$ inclusions while there are only little MgF_2 inclusions. If the amount of MgF_2 in the slag is raised to 5.0 wt.-% a significant drop of CaF_2 inclusions takes place. Simultaneously, the amount and distribution of $CaF_2 + MgF_2$ and MgF_2 inclusions is kept constant. By a further increase of MgF_2 up to 10.0 wt.-% a further decrease of CaF_2 inclusions can be achieved. However, this decrease is combined with a raise of both $CaF_2 + MgF_2$ and MgF_2 inclusions. This is reflected not only by the amount but also by the size of the inclusions. Figure 11 c) shows that the amount of $CaF_2 + MgF_2$ inclusions with a size of 2.5 to 5.0 µm is approximated progressively to the amount of $CaF_2 + MgF_2$ inclusions with a size of 1.0 to 2.5 µm.

The slag has been analyzed on its CaF_2, MgF_2, TiO_2 and Al_2O_3 content. It has been observed, that there was only little deviation of the TiO_2 and Al_2O_3 content in the cap slag, the slag skin and the fly dust if the MgF_2 content in the process slag system was

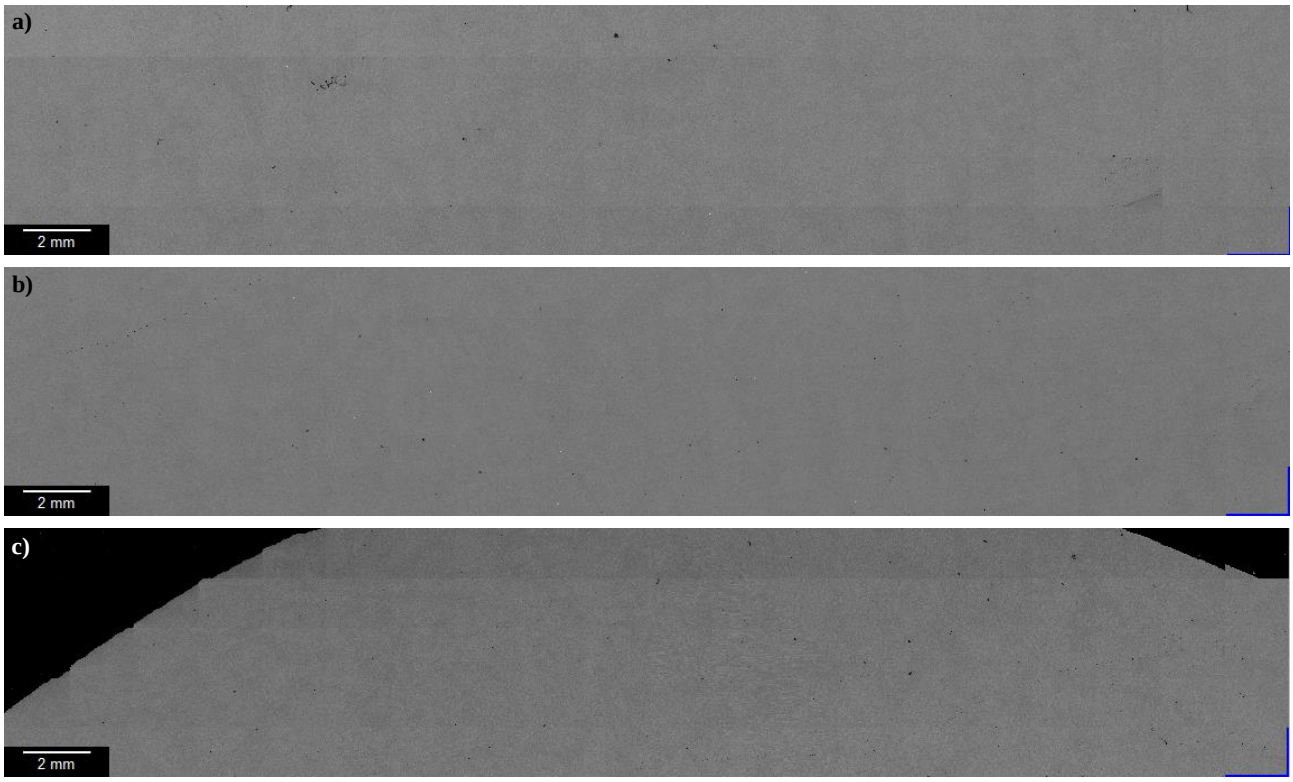

Figure 10: Measuring field for non-metallic inclusions by energy-dispersive X-ray microanalysis; a) Trial A: 2052 + 2.5 wt.-% MgF_2, b) Trial B: 2052 + 5.0 wt.-% MgF_2, c) Trial C: 2052 + 10.0 wt.-% MgF_2

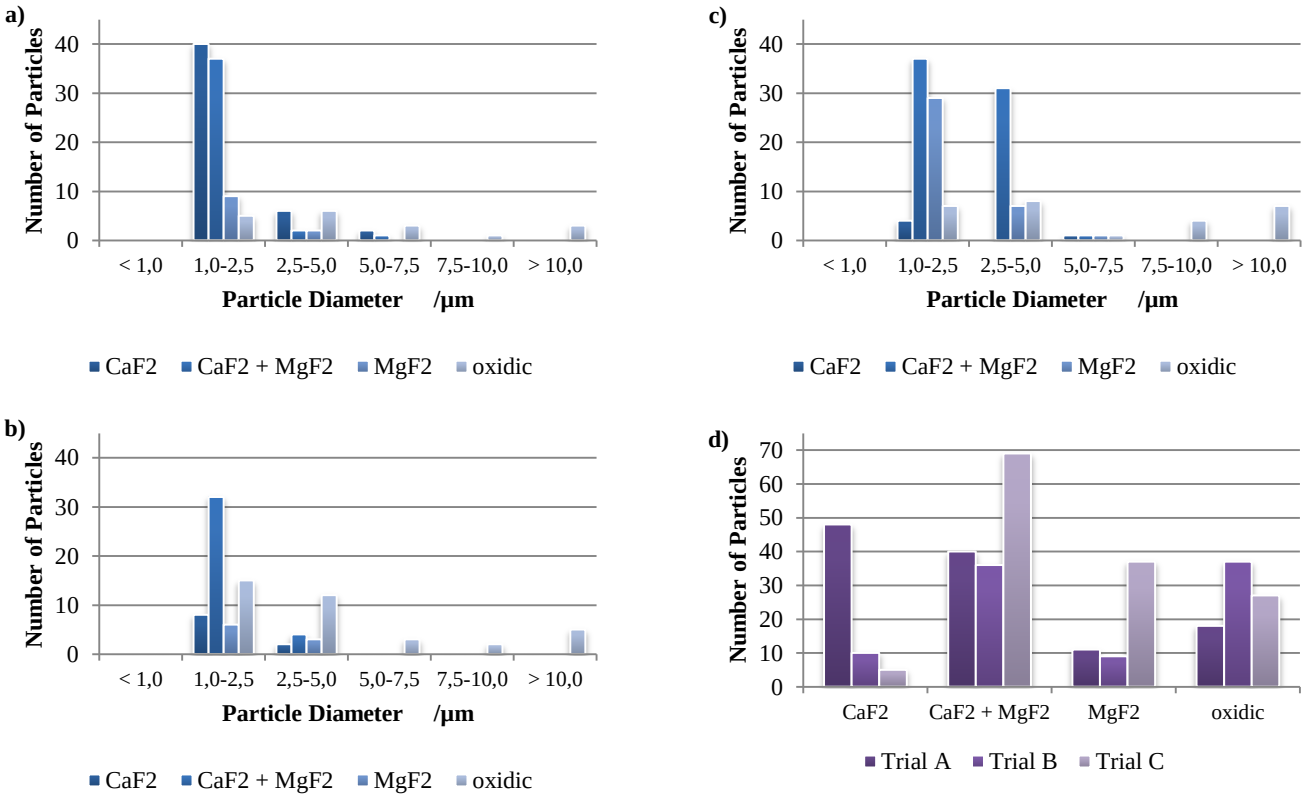

Figure 11: Non-metallic inclusions analyzed by XRD analysis divided according to size (a) Trial A: 2052 + 2.5 wt.-% MgF_2, b) Trial B: 2052 + 5.0 wt.-% MgF_2, c) Trial C: 2052 + 10.0 wt.-% MgF_2) and total number (d))

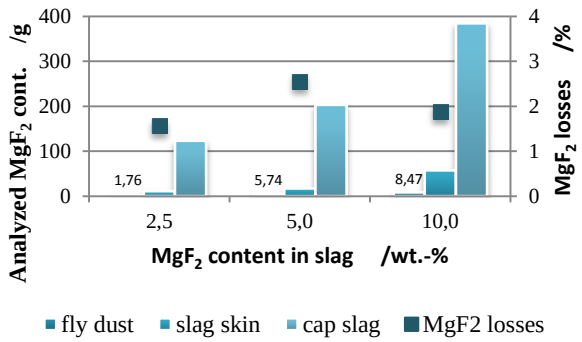

Figure 12: Consideration of MgF_2 losses during remelting in regard to different slag compositions

changed. The CaF_2 content changed as expected and was lower if the MgF_2 content was raised. Considering the MgF_2 content it could be seen that the MgF_2 losses by evaporation and fly dust show almost no context with an increasing MgF_2 content in the process slag. It can be assumed that these losses occur during the initial phase due to higher temperatures and turbulences because of arcing.

Conclusion

(1) Minor variations of the ingot homogeneity can be achieved by remelting pressed electrodes once. An improvement might be possible by changing the electrode morphology.

(2) The partial substitution of CaF_2 by MgF_2 leads to a minor fluorine absorption in TiAl. Nevertheless, by increasing the amount of MgF_2 it appears that the fluorine pickup levels off and no significant fluorine contents can be achieved.

(3) The slag system has almost no influence on the amount and size of oxidic NMI, the influence on fluoridic inclusions is significant. By increasing the MgF_2 content in the slag it is possible to reduce CaF_2 inclusions. However, if the MgF_2 content is too high, the size and number of both $CaF_2 + MgF_2$ and MgF_2 inclusions are raised.

(4) Due to the constant initial phase a MgF_2 loss of around 2 wt.-% cannot be avoided, but on the other hand is not exceeded even with high MgF_2 contents in the slag system.

Outlook

The present work shows that a partial substitution of CaF_2 by MgF_2 leads to no significant absorption of fluorine in Ti-45Al. Nevertheless, a raise of the fluorine content can be achieved by raising the MgF_2 content in the process slag. Therefore, in further investigations a raise of MgF_2 to 100 wt.-% as well as the use of NaF_2 will be considered (ΔH_{MgF_2}: -1124.2 kJ/mol; ΔH_{NaF}: -572.8 kJ/mol). Furthermore, electrodes with decreased aluminum content will be used to investigate the influence of aluminum on the fluorine absorption.

References

1. Boeing Long-Term Market Outlook 2013-2032 http://active.boeing.com/commercial/forecast_data/index.cfm, January 2014
2. H. Clemens, "Intermetallische Werkstoffe für Anwendungen in Automobil- und Flugzeugtriebwerken," *BHM Berg- und Hüttenmännische Monatshefte*, 153 (2008), 337-341
3. S. Knippscheer, and G. Frommeyer, „Neu entwickelte TiAl-Basislegierungen für den Leichtbau von Triebwerks- und Motorenkomponenten – Eigenschaften, Herstellung, Anwendung," *Materialwissenschaft und Werkstofftechnik*, 37 (2006), 724-730
4. E.A. Loria, "Quo vadis gamma titanium aluminide," *Intermetallics*, 9 (2001), 997-1001
5. P.J. Masset, "Influence of alloy compositions on the halogen effect in TiAl alloys," *Materials and Corrosion*, 59 (2008)
6. M. Schütze, "The halogen effect in the oxidation of intermetallic titanium aluminides," *Corrosion Science*, 44 (2002)
7. A. Donchev, "Improvement of the oxidation behavior of TiAl-alloys by treatment with halogens," *Intermetallics*, 14 (2005), 1168-1174
8. A. Donchev et al., "Optimization of the fluorine effect for improving the oxidation resistance of TiAl-alloys," *Materials Science Forum*, 706-709 (2012), 1061-1065
9. H.-E. Zschau et al., "Surface Modification by Ion Implantation to Improve the Oxidation Resistance of Materials for High Temperature Technology," *Ion Implantation*, 17 (2012), 409-436
10. J. Reitz et al., "Recycling of gamma titanium aluminide scrap from investment casting operations", *Intermetallics*, 19 (2011), 762-768
11. R.H. Nafziger, "Slag compositions for Titanium Electroslag Remelting and Effects of Selected Malting Parameters", *Proceedings of Second International Symposium on Electroslag Remelting Technology*, (1969)
12. H. Scholz et al., "An Advanced ESR Process for the Production of Ti-Slabs", *Ti-2003 Science and Technology*, ed. G. Lütjering and J. Albrecht (Weinheim, Wiley-VCH-Verlag, 2004), 205-212
13. P. Spiess, "Experimental Research on the Absorption of Fluorine in gamma-TiAl during Electroslag Remelting," *Proceedings of the 2013 International Symposium on Liquid Metal Processing and Casting*, (2013), 65-70
14. B.I. Medovar, "Electroslag remelting of alloy steel," *Metallurg*, 4 (1970), 32-35
15. N. Giesselmann et al., "Numerical simulation of the electroslag remelting process in order to determine influencing parameters on ingot defects," *Proceedings of the 1st International Conference on Ingot Casting, Rolling and Forging*, (2012)
16. B. Friedrich, C. Lochbichler, and J. Reitz, „Closing The Material Cycle of Titanium – Thermochamical and Experimental Validation of a New Cycling Concept," *Proceedings of the 2007 International Symposium on Liquid Metal Processing and Casting*, (2007)